

Deuteration of Water in Protoplanetary Disks During Luminosity Outbursts: Model Predictions for FU Ori Disks

Anastasiia Topchieva^{1,2}, Tamara Molyarova³, and Anton Vasyunin²

Institute of Astronomy, Russian Academy of Sciences, Pyatnitskaya St. 48, Moscow, 119017, Russia; ATopchieva@inasan.ru

Ural Federal University named after the first President of Russia B.N. Yeltsin, Mira Av. 19, Yekaterinburg, 620002, Russia

Research Institute of Physics, Southern Federal University, Rostov-on-Don, Russia

Received 2025 July 15; revised 2025 September 17; accepted 2025 October 16; published 2025 November 14

Abstract

Luminosity outbursts of FU Ori-type objects (FUors) allow us to observe in the gas the molecules that are typically present in the ice in protoplanetary disks. In particular, the fraction of deuterated water, which is usually mostly frozen in the midplane of a protoplanetary disk, has been measured for the first time in the gas of the disk around FUor V883 Ori. We test the hypothesis that the observed high HDO/ $\rm H_2O$ ratio in the V883 Ori protoplanetary disk can be explained by luminosity outbursts of different amplitude, including a series of two consecutive outbursts. Using the ANDES astrochemical code, we modeled the distributions of water and deuterated water abundances under the action of luminosity outbursts of different amplitudes (from 400 to $10,000\,L_\odot$) and at different stellar luminosities at the pre-outburst stage. We show that the best agreement with the observed HDO/ $\rm H_2O$ profile is obtained for outburst amplitudes of 2000 and $10,000\,L_\odot$, while the observed bolometric luminosity of V883 Ori does not exceed $400\,L_\odot$. We discuss possible reasons for this discrepancy, including the presence of past luminosity outbursts, the age of the star, and the influence of additional heating mechanisms in the midplane of the protoplanetary disk. We also consider how the high observed HDO/ $\rm H_2O$ ratio may be related to the evolution of the chemical composition of the ice in the protoplanetary disk and the chemical processes activated under outburst conditions.

Key words: astrochemistry – interplanetary medium – protoplanetary disks

1. Introduction

The study of the water ice in protoplanetary disks is key to understanding the origin of water in planetary systems, including the Earth (Kirsanova et al. 2025). Water in protoplanetary disks plays a key role in the chemical evolution and formation of planets (Drążkowska & Alibert 2017; Müller et al. 2021). Accretion outbursts, such as those observed in FU Ori-type stars (FUors), can significantly affect the distribution of water and its deuterated form (HDO). The chemistry of deuterated species differs from that of the main isotopologues. Being sensitive to values of medium temperature and density as well as radiation, the ratio between H₂O and HDO abundances must evolve during star formation from the interstellar cloud to the protoplanetary disk and the forming planetesimals and planets (Cleeves et al. 2014; Furuya et al. 2016).

The modeling results show that during luminosity outbursts, the temperature in the protoplanetary disk increases dramatically, leading to the evaporation of water ice and a change in the $\rm HDO/H_2O$ ratio in the gas phase. This can be reflected in the observed spectra, providing information on the dynamics and chemistry of the protoplanetary disk (Wiebe et al. 2019; Tobin et al. 2023). In particular, a high $\rm HDO/H_2O$ ratio may

indicate the origin of water in the cold molecular phase before star formation, while its decrease is possibly due to thermal processing in the hot inner regions of the protoplanetary disk (Jacquet & Robert 2013; Tobin et al. 2023).

Modern interferometric observations allow us to study the spatial distribution of HDO and H_2O in the disks and envelopes of young protostars. In particular, for Class 0 and Class I objects, such as V883 Ori and L1551 IRS5, the HDO/ H_2O ratios obtained from observations reach $(2.1-2.3)\times 10^{-3}$, which is significantly higher than the values typical of terrestrial oceans ($\sim 1.6\times 10^{-4}$) and comparable to the observed values in comets (Andreu et al. 2023; Tobin et al. 2023). These results support the hypothesis of "inherited" water that has passed from the molecular cloud into the protoplanetary disk without significant chemical processing.

At present, the evolution of the HDO/ H_2O ratio under conditions of variable luminosity remains an open question. FUors, which V883 Ori and L1551IRS5 are examples of, undergo accretion outbursts accompanied by a sharp increase in luminosity to hundreds or thousands of L_{\odot} .

Observations of the V883 Ori protoplanetary disk in the HDO emission line show that the water snow line is located at a distance of \sim 80 au from the star (Tobin et al. 2023). Indirect

methods give different but also high values for this distance: \sim 40 au from dust emission from Cieza et al. (2016) which was not confirmed in later multiwavelength observations by Houge et al. (2023), and \sim 100 au from HCO⁺ Leemker et al. (2021). At the same time, under the standard luminosity of the star (\lesssim 10 L_{\odot}), the position of the snow line is expected to be no more than a few au away, and even when the luminosity increases to \sim 400 L_{\odot} , radiative heating is able to shift the water snow line to a maximum distance of \sim 20 au (Harsono et al. 2015). This discrepancy suggests that residual heating from previous outbursts or additional mechanisms of heat redistribution, such as non-radiative heating in the midplane of Alarcón et al. (2024), need to be taken into account.

Although early models of Furuya et al. (2013), Bergin et al. (2007) show that vertical mixing and photochemistry play an important role in the redistribution of HDO/H_2O in the protoplanetary disk, they did not consider the influence of FUor luminosity outbursts, whose brief heating can also cause changes in the relative abundance of deuterated water (Owen & Jacquet 2015). We consider a scenario in which it is luminosity outbursts, rather than slow mixing processes, that are the key factor in shaping the observed deuterated water distribution.

In the present work, we investigate the effect of accretion outbursts on the evolution of the HDO/H_2O ratio in protoplanetary disks. The distributions of water and its deuterated form at different luminosity levels (400–10,000 L_{\odot}) are modeled using the ANDES astrochemical code to reproduce conditions before, during and after the outburst. Special attention is paid to the following aspects:

- 1. whether the outburst can explain the observed high HDO/H₂O;
- 2. how the radial distribution of HDO/H₂O changes due to the outburst;
- 3. how much the position of the water snow line and the HDO/H₂O distribution depend on the outburst amplitude and the presence of additional heating mechanisms;
- 4. and to what extent the observed HDO/H_2O ratio reflects the composition of the original ice, or has undergone reprocessing during chemical evolution.

Our goal is to try to explain the existing Atacama Large Millimeter/submillimeter Array (ALMA) data for V883 Ori and to determine which outburst scenario is most consistent with the observed HDO/ H_2O ratio. In addition, we aim to establish a link between conditions in protoplanetary disks around FUors and the chemical composition of ice in the early the solar system, including data from comets. This will improve our understanding of the role of accretion outbursts in the evolution of molecular composition and help to refine scenarios for the transport of water to Earth-like planets.

The paper is organized as follows. Section 2 describes the numerical model and calculation parameters. Section 3 presents

the HDO/H₂O radial profiles for different outburst scenarios. Section 4 discusses possible reasons for the discrepancy between models and observations, as well as the possible evolution of HDO/H₂O from the protoplanetary disk formation to the present-day solar system. In Section 5, we formulate the main conclusions regarding the effect of outbursts on the chemistry of water ice in protoplanetary disks.

2. Model

2.1. Observed Parameters of the V883 Ori System and Modeling the Protoplanetary Disk Structure

In our modeling, we rely on the observed characteristics of the V883 Ori system. It has been observed many times with ALMA and other instruments, which allowed us to obtain estimates of its main parameters (Cieza et al. 2016, 2018). The star has a mass of about 1.3 M_{\odot} , a protoplanetary disk radius of 67–370 au, and a protoplanetary disk mass of $0.2-0.38 M_{\odot}$, according to data from Kóspál et al. (2021). According to these data, the protoplanetary disk is quite massive: 20%-50% of the mass of the central star, suggesting the possibility of gravitational instability. However, spatially resolved observations of dust emission show no evidence of asymmetric substructures characteristic of advanced gravitational instability (Cieza et al. 2016). Newer observations indicate a lower value of the protoplanetary disk mass of $0.02-0.09 M_{\odot}$ (Schoonenberg et al. 2017; Tobin et al. 2023), which is in better agreement with the absence of substructures in the disk. In the model, the mass of the protoplanetary disk is assumed to be $0.05\,M_{\odot}$, and the characteristic radius is assumed to be 125 au.

The bolometric luminosity of V883 Ori is about $400 L_{\odot}$ (Sandell & Weintraub 2001). With newer distance measurements, the luminosity estimates are updated, e.g., 200 L. reported by Furlan et al. (2016) and 460 L⊙ reported by Carvalho et al (2025). We will rely on a conservative estimate of the current luminosity of $400 L_{\odot}$. As indicated by Strom & Strom (1993), a brighter nebula around this star was observed as early as in 1888 by Pickering (1890), indicating that the outburst started back then (see, for example, Connelley & Reipurth 2018; Tobin et al. 2023). We will assume that the duration of the outburst is \sim 130 yr. The age of the star is estimated to be about 0.5 Myr; it belongs to Class I of young stellar objects because it retains an envelope mass comparable to the mass of the protoplanetary disk (Evans et al. 2009; Cieza et al. 2016). Indirect observations of the snow line in this protoplanetary disk at a large distance from the star suggest that the luminosity may have been higher in the past (Leemker et al. 2021). This is also indicated by historical observations of a brighter nebula in the vicinity of this star (Connelley & Reipurth 2018). We therefore consider different scenarios for the luminosity change described below in Section 2.3.

We use the ANDES astrochemical code (Akimkin et al. 2013) to study the chemical evolution of the protoplanetary disk under the influence of the FUor outburst. The structure of the disk is constructed following the model presented in Molyarova et al. (2017). The protoplanetary disk is assumed to be axisymmetric, and the surface density distribution is described by a power law. The vertical structure is calculated from the hydrostatic equilibrium conditions.

The temperature of the protoplanetary disk, both in the radial and vertical directions, is determined using a combined method: for the atmosphere, the UV radiative transfer calculation is used, while the temperature in the midplane is determined parametrically based on the total source luminosity (stellar and accretion) (Williams & Best 2014; Isella et al. 2016; Molyarova et al. 2017). The density and temperature distributions are calculated iteratively until mutual agreement is achieved. We assume that dust and gas temperatures are equal, which is a reasonable approximation in the collisionally dominated disk midplane (Kamp & Dullemond 2004; Woitke et al. 2009). The optical properties of the dust are adopted from Laor & Draine (1993), with the dust mass assumed to be 1% of the gas mass. We assume a power-law size distribution of dust grains with a -3.5 exponent and minimum and maximum dust grain sizes $a_{\min} = 5 \times 10^{-7} \,\mathrm{cm}$ and $a_{\max} = 2.5 \times 10^{-3} \,\mathrm{cm}$, which correspond to slightly grown dust compared to the standard values for the interstellar medium. Luminosity outburst could affect dust size in the disc around V883 Ori, and ALMA observations do show evidence of dust growth (Houge et al. 2023; Houge and Krijt 2023), which could affect chemistry and should be considered in a separate study. A more detailed description of the dust model is given in Section 2.2 of Molyarova et al. (2018).

In order to model a Class I object, it is necessary to take into account the surrounding envelope in addition to the protoplanetary disk itself. We consider a model based on the work of Whitney et al. (2003), which describes the density distribution in a rotating accreting envelope. A more detailed implementation of the envelope in the ANDES model and its influence on the chemistry of FUors is described in Molyarova & Elbakyan (2019), Zwicky et al. (2024). The main parameters of the envelope in the model are the outer radius (1000 au), the accretion rate through the envelope $10^{-5} M_{\odot} \text{ yr}^{-1}$, and the centrifugal radius equal to the characteristic radius of the protoplanetary disk 125 au. With the parameters given in the model, the total mass of the envelope is $0.026 M_{\odot}$.

2.2. Chemical Model

To describe the chemical evolution of deuterated water, we use a chemical reaction network that includes deuterium fractionation (Semenov & Wiebe 2011; Albertsson et al. 2013). It includes 1247 chemical components and 38,347 reactions, including gas-phase and surface two-body reactions,

adsorption and reactive desorption, photoreactions, ionization and dissociation by X-rays, cosmic rays and radioactive nuclides (see, for example Woitke et al. 2009; Akimkin et al. 2013). The considered set of species includes mono-, di-, and trideuterated molecules and ions, including those on dust surface. The model also includes ortho- and para-isomers of molecular hydrogen, which are necessary to correctly describe the chemistry of deuterated species.

The model is optimized and tested for the cold conditions of the interstellar medium and reproduces well the chemistry of deuterated species at temperatures below 150 K (Albertsson et al. 2013). We suggest that the water vapor composition observed in the protoplanetary disk around V883 Ori is mainly determined by the composition of the ice evaporated by the luminosity outburst. Gas-phase two-body reactions for higher temperatures are available in the reaction network and are accounted for by temperatures up to 600 K. Also included in the grid are photoreactions that can influence the dissociation of water in the molecular layer. However, it should be noted that the results of calculations in the inner protoplanetary disk and at temperatures above 600 K are less reliable. This feature of the model nevertheless does not prevent comparison with the observed composition of the protoplanetary disk: spatially resolved data for the radial concentrations of water isotopologues are obtained for distances >40 au, and the temperature in the protoplanetary disk midplane at this distance does not exceed 250 K even at a luminosity of $10,000 L_{\odot}$.

As an initial chemical composition, we use the composition of ices observed in protostellar cores (Öberg et al. 2011; Eistrup et al. 2016), where molecular ices of the main volatile species are present. At the initial time instant, deuterium is present only in the gas phase as part of the HD molecule, with its initial abundance being 1.55×10^{-5} with respect to hydrogen nuclei. This value corresponds to the observed deuterium abundance in the interstellar medium (Wilson & Rood 1994).

2.3. Luminosity Outburst Model

We evolve disk physical structure due to the effect of an outburst following the approach from Molyarova et al. (2018). The total luminosity of the central source consists of the intrinsic stellar luminosity and the accretion luminosity, which changes throughout the outburst. Changes in the total luminosity are reflected in the vertical structure of the disk, which is recalculated at each new luminosity value. In this work, we do not consider the hydrodynamical response of the protoplanetary disk to the outburst and assume that the structure adapts instantaneously to the change in luminosity. As the accretion luminosity increases, the protoplanetary disk heats up, thickens, and becomes more inflated. It should be noted that the models are quasi-stationary and not all regions of the protoplanetary disk manage to reach an equilibrium state

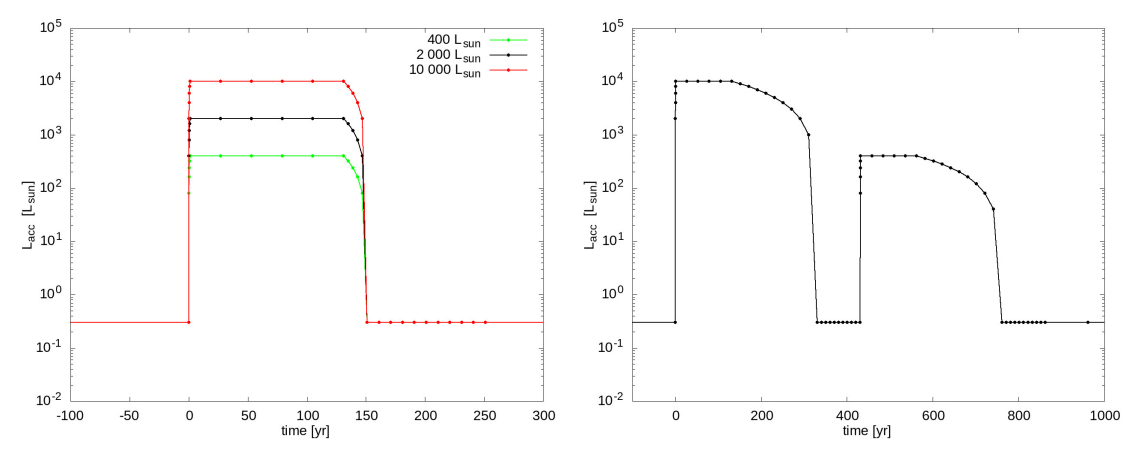


Figure 1. Evolution of the total luminosity of the accretion source in different models. Three models with different outburst amplitudes: 400, 2000, and 10,000 L_{\odot} are shown on the left. On the right is the model with two consecutive outbursts with amplitudes of 10,000 and 400 L_{\odot} . The time is specified relative to the outburst onset.

within a typical outburst time (on the order of 100 yr), see, e.g., Equations (24)–(30) in Chiang & Goldreich (1997) or Figure 3 in Vorobyov et al. (2014). The effects of thermal inertia and gas dynamics are not accounted for in the current model; inclusion of these processes may further shift the snow line in the late stages of the outburst (see Vorobyov et al. 2014).

We assume that the outburst lasts 130 yr, based on the observed duration of the V883 Ori outburst (Connelley & Reipurth 2018). Before the onset of the outburst, the accretion luminosity remains unchanged at $0.3\,L_\odot$, which is a typical value for young T Tauri-type stars. With the onset of the outburst, the luminosity rises to its maximum amplitude during one year. We consider outbursts with amplitudes of 400, 2000, and $10,000\,L_\odot$, as well as the case where two consecutive outbursts occur. The luminosity is assumed to have a maximum value for 130 yr, after which it declines to a preoutburst level for 20 yr. Model profiles of the evolution of the accretion luminosity for several models with different peak luminosities are shown in Figure 1.

In the pre-outburst phase, the star is the main contributor to the luminosity. Ages of young stars are not precisely measured, but luminosity of the star during the pre-outburst period can influence the composition of the ice exposed by the outburst. The age of V883 Ori is considered to be ≈ 0.5 Myr (see Cieza et al. 2016), but this estimate is based mainly on the presence of a surrounding envelope and thus the object belonging to Class I. Estimates of the duration of the evolutionary stages of young stars show that they may be in the Class 0 stage for ~ 0.1 Myr and in the Class I stage for ~ 0.5 Myr (Evans et al. 2009). The luminosity of a star L_{\star} with the adopted mass of $1.3 \, M_{\odot}$ is $\sim 17 \, L_{\odot}$ at an age of 0.1 Myr and $\sim 5 \, L_{\odot}$ at an age of 0.5 Myr, according to the evolutionary tracks from the Yorke & Bodenheimer (2008) model. We consider models with these two values of stellar luminosity.

 Table 1

 Modeling Parameters for Accretion Outbursts

| No | $L_{ m acc},L_{\odot}$ | Features |
|----|------------------------|---|
| 1 | 400 | Single outburst, observed amplitude |
| 2 | 2000 | Single outburst, increased amplitude |
| 3 | 10,000 | Single outburst, maximum amplitude |
| 4 | 10,000 + 400 | Two consecutive outbursts (100 yr apart): first |
| | | $10{,}000L_{\odot}$, then $400L_{\odot}$ |

However, we do not consider different values of the outburst duration. As shown in Wiebe et al. (2019), for outbursts longer than 100 yr, the outburst duration does not significantly affect the chemical composition of the disk.

Table 1 presents the parameters of the numerical models of accretion outbursts used in this work.

For each model, the time interval before its onset is $\Delta t = 0.5$ Myr, and two values of the stellar luminosity are considered. We consider both single outbursts with different amplitudes and time intervals before the onset of the outburst, as well as a scenario with two consecutive outbursts.

3. Results

3.1. Water Snow Line Position

The temperature in the disk plane $T_{\rm mp}$ depends on the luminosity of the central source and increases during the accretion burst. In the model, it is calculated from the temperature and size of the star and the accretion region:

$$T_{\rm mp}^4(R) = \frac{\alpha}{2} \left(T_{\star}^4 \left(\frac{R_{\star}}{R} \right)^2 + T_{\rm acc}^4 \left(\frac{R_{\rm acc}}{R} \right)^2 \right). \tag{1}$$

Here $\alpha = 0.05$ is the angle between the surface of the protoplanetary disk and the light beam from the central source.

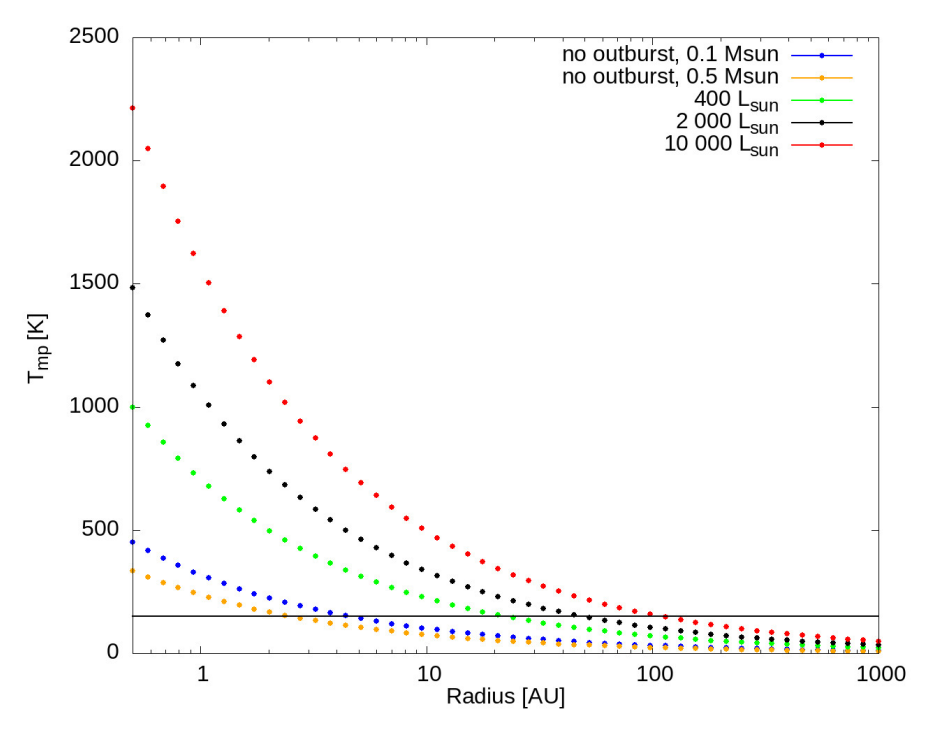


Figure 2. Temperature in the protoplanetary disk midplane with no outburst for stellar ages of 0.1 and 0.5 M_{\odot} and at different values of accretion luminosity. The horizontal black line indicates the sublimation temperature of water ice (\approx 150 K). The intersections with it of the dashed temperature profiles correspond to the approximate position of the water snow line at the given luminosities.

This temperature profile describes an optically thick protoplanetary disk with an inner hole illuminated by a central source (Chiang & Goldreich 1997; Dullemond et al. 2001).

The stellar temperature T_{\star} and the stellar radius R_{\star} in the model are set according to the evolutionary tracks from Yorke & Bodenheimer (2008) and correspond to the stellar luminosities of ≈ 5 and $\approx 17\,L_{\odot}$ for the two considered stellar ages. The temperature of the accretion region is assumed to be $T_{\rm acc}=10{,}000\,\rm K$, and the radius is set based on a given value of accretion luminosity $L_{\rm acc}=4\pi R_{\rm acc}^2\,\sigma_{\rm SB}T_{\rm acc}^4$, which varies with time (see Section 2.3). If we assume that the accretion luminosity is much larger than the luminosity of the star, which is true for the considered outbursts of luminosities $>100\,L_{\odot}$, we obtain $T_{\rm mp}(R)\sim L_{\rm acc}^{1/4}R^{-1/2}$ during the outburst. We further discuss an alternative temperature profile in Section 3.4.

During a luminosity outburst, the water snow line shifts further away from the star. Figure 2 shows the radial temperature distribution in the midplane under different conditions: in the absence of an outburst (before its onset) for stellar ages of 0.1 and $0.5\,M_\odot$ and during an outburst with different luminosities. The characteristic sublimation temperature of water ice in protoplanetary disks is $\approx 150\,\mathrm{K}$, although this value depends on local environmental conditions, in particular on the gas density (Harsono et al. 2015). The position of the water snow line in the midplane can be

estimated as the distance at which the temperature is equal to this value. Above the midplane, temperatures are typically higher, and the snow line moves further away from the star and becomes a snow surface. However, observations of optically thin water emission allow us to determine the position of the snow line in the disk midplane (Tobin et al. 2023), so we focus on this temperature.

As can be seen from Figure 2, at the quiescent stage the water snow line is at a distance of $\sim 2-5$ au, and it shifts to $\sim 20-100$ au during an outburst. At the observed luminosity of V883 Ori $<400\,L_\odot$, the water snow line could be at a distance of ~ 20 au (green dashed line in the Figure 2) if its position is determined only by radiative heating from the luminosity outburst. The distances 40-100 au obtained from observations (Cieza et al. 2016; Leemker et al. 2021; Tobin et al. 2023) should only be expected in this case for a much larger luminosity outburst, such as the 2000 or $10,000\,L_\odot$ shown here.

Figure 3 shows the distributions of the relative abundances of $\rm H_2O$ and HDO in the gas and solid phases as a function of the distance to the star for models with three different outburst amplitudes (400, 2000, and $10,000\,L_\odot$) and two stellar ages (0.1 and 0.5 Myr). The dotted lines correspond to the abundance in the gas phase, the solid lines show the ice on dust grain surface. During a $10,000\,L_\odot$ outburst (red lines), the temperature is so high that almost all water is converted to the gas phase and no snow line forms. For outbursts of 2000 and

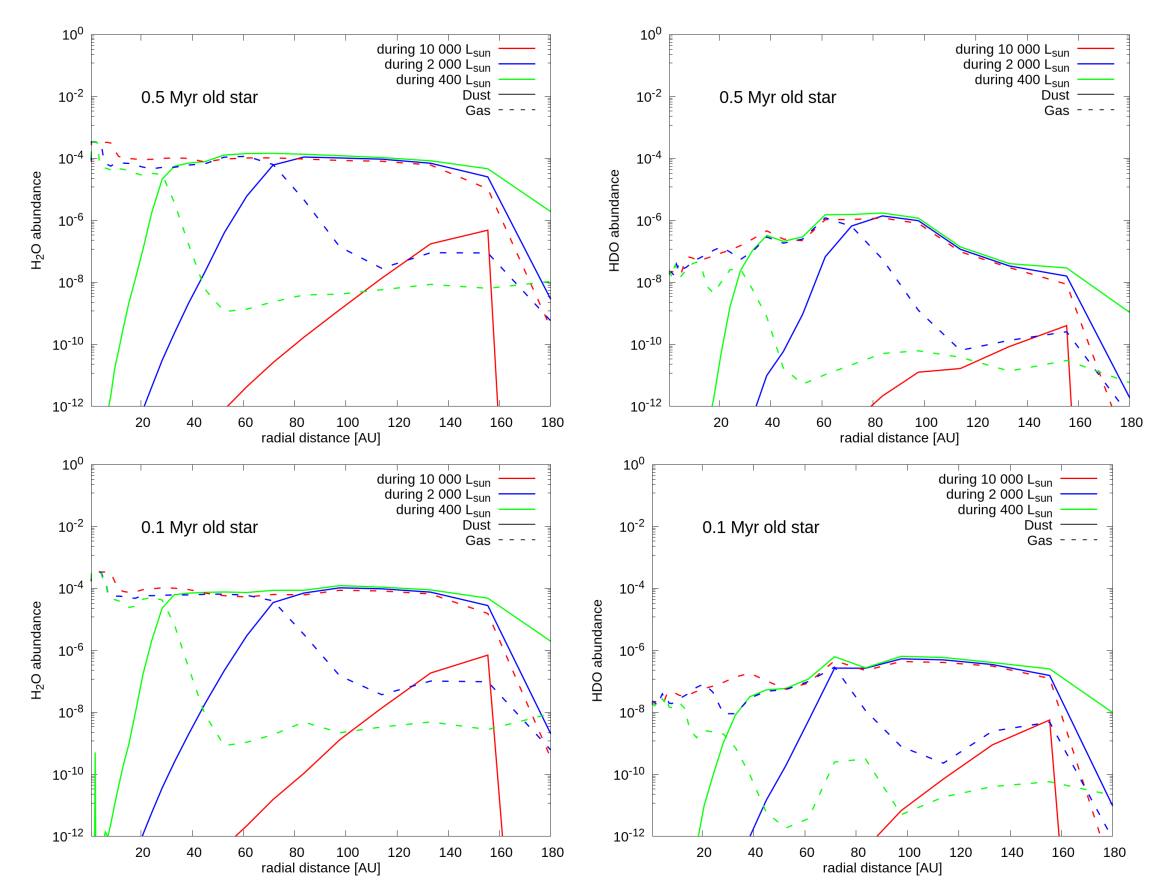


Figure 3. Relative water abundance in the gas and on dust grain surface (in the ice) at different accretion luminosities (400, 2000, and 10,000 L_{\odot}) for stellar ages of 0.1 and 0.5 Myr. The red, green, and blue colors signify outbursts with luminosities of 10,000, 2000, and 400 L_{\odot} , respectively. The intersection of ice and gas components defines the snow line. At 10,000 L_{\odot} (red), the ice abundance is low and the H₂O and HDO snow lines are absent. For fainter outbursts, the snow lines are at 20–30 au (400 L_{\odot} , blue) and ~70 au (2000 L_{\odot} , green).

 $400\,L_\odot$, characteristic intersections of the gas and solid components corresponding to the snow line positions are observed: about $20-30\,\mathrm{au}$ for $400\,L_\odot$ and $60-70\,\mathrm{au}$ for $2000\,L_\odot$.

In addition to thermal desorption, the adopted astrochemical model also includes photodesorption, which leads to the evaporation of water in the outer regions of the protoplanetary disk more transparent for UV radiation. It reduces the ice abundance at distances \gtrsim 120 au. In addition, the model is twodimensional (R, z), that is, it considers the structure of the protoplanetary disk in the vertical direction, and the radial profiles shown in Figure 3 are obtained by integration in the vertical direction. The freeze-out temperature of water in the upper layers of the protoplanetary disk is reached at greater distances from the star than in the midplane. When considering the full vertical span of the disk, it results in a shift of the snow line further away from the star and a smoother change in the gas and dust abundances in the vicinity of the snow line. In addition, the chemical kinetics model takes into account that the extinction rate depends on the gas density, and the freezeout temperature can differ from the standard value of 150 K. The combination of these factors causes the snow line positions in the astrochemical model (Figure 3) to differ slightly from the estimate based on the freeze-out temperature (Figure 2).

The observed position of the snow line in the disk midplane at a distance of 40-100 au corresponds to a luminosity of the order of $10^3 - 10^4 L_{\odot}$ and cannot be obtained at the current luminosity of $400 L_{\odot}$ in the absence of heating mechanisms other than radiation heating and in a quasi-stationary disk. Perhaps, in the past, the snow line was shifted to these distances by a brighter outburst and has not since had time to come into agreement with the current luminosity due to the finite time of establishing the thermal balance. Different physical and chemical processes in the protoplanetary disk occur on different timescales, which may also explain the inconsistency of the snow line positions determined by different methods (from dust properties in Cieza et al. 2016, from the emission of the chemical tracer HCO⁺ in Leemker et al. 2021, from the emission of water isotopologues in Tobin et al. 2023). In the following section, we use astrochemical modeling to test whether the observed HDO/H₂O ratio is

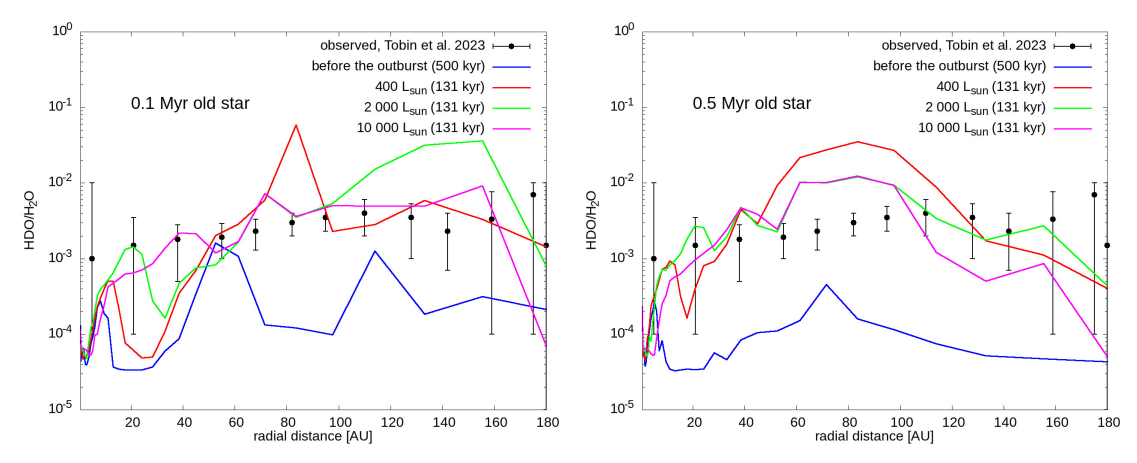


Figure 4. Radial profiles of the HDO/H₂O ratio in the gas for different outburst scenarios. Black marks with error bars show observational data for the V883 Ori protoplanetary disk from Tobin et al. (2023), with values inside 40 au considered less reliable due to the contribution of the optically thick dust continuum. The blue line corresponds to the time before the outburst (t = 500 kyr). The red, green, and magenta lines show the simulation results 131 yr after the outburst at different maximum luminosities: $400 L_{\odot}$, $2000 L_{\odot}$, and $10,000 L_{\odot}$, respectively.

consistent with different outburst scenarios and whether, like the position of the water snow line, it indicates a brighter outburst.

3.2. Comparing Models with Different Luminosities

The model allows us to calculate the two-dimensional (R, z) distribution of molecules in the protoplanetary disk evolving in time. We are interested in the ratio between the gas-phase abundances of the water isotopologues HDO and $\rm H_2O$, namely, a comparison of this ratio with the observational data from Tobin et al. (2023). Since the observations are spatially resolved only in the radial direction, we integrate the HDO and $\rm H_2O$ abundances over z, and consider the radial profiles of the $\rm HDO/H_2O$ ratio in comparison with the observations.

Figure 4 compares the radial profiles of the HDO/H₂O ratio before and during the outburst in models with different peak luminosities and for two stellar ages (0.1 and 0.5 M_{\odot}). Prior to the outburst (500 kyr time point, blue line in the Figure 4), the model predicts relatively low HDO/H₂O values across the disk. This ratio is determined mainly by molecules in the upper layers of the disk, where water (both H₂O and HDO) is in the gas phase due to photodesorption and higher temperatures. At the same time, most of water is in the disk midplane in the form of ice mantles on the dust surface and does not contribute to the integrated gas-phase HDO/H₂O. During an outburst, this water ice evaporates; the region of the protoplanetary disk where this occurs depends on the brightness of the outburst. However, at all values of the maximum luminosity, water ice in both the upper layers of the protoplanetary disk and in the midplane will transition to the gas phase, consequently leading to a change in HDO/H₂O at all distances from the star. The water ice in the disk midplane evaporates and completely turns into the gas inside the water snow line (see Figure 3). At distances \gtrsim 40 au, the abundance of both H₂O and HDO in the gas phase at high luminosities almost completely coincides with the abundance of the corresponding ice at lower luminosities. This means that the gas-phase HDO/H_2O ratio within the snow line during the outburst is determined mainly by the ice composition before the outburst.

At 131 yr, when the model luminosity is still at its maximum value (see Figure 1), the HDO/H₂O ratio is elevated compared to the pre-outburst. This is particularly pronounced in the high peak luminosity models of $2000L_{\odot}$ and $10,000\,L_{\odot}$. These models show better agreement with the observational data in the 60–100 au. The model with an outburst amplitude of $400\,L_{\odot}$ shows a lower HDO/H₂O ratio in this region, except for a peak occurring at \approx 80 au for a 0.1 Myr old star. The model with $400\,L_{\odot}$ also has a higher hump in the region of 40–130 au than models with $2000\,L_{\odot}$ and $10,000\,L_{\odot}$ outburst, for stellar ages of 0.5 Myr. This also supports the hypothesis of a brighter luminosity outburst in V883 Ori.

In the inner disk, at r < 40 au, models with bright outbursts also demonstrate better agreement with observational data. However, as Tobin et al. (2023) point out, at these distances, dust emission is optically thick. This can lead to significant distortions in observed column densities and, consequently, to a more inaccurate observational HDO/H₂O ratio. When comparing models with observations, only distances greater than 40 au should be considered.

To interpret the local increase in the HDO/H_2O ratio during outbursts of different brightness, we analyzed the chemical reactions contributing to the change in the HDO abundance in the gas phase. In the bulk of the disk, it is driven by ice evaporation and reflects the available HDO/H_2O in the ice phase in the protoplanetary disk prior to the outburst. However, there are also gas-phase reactions with different efficiencies for HDO and H_2O that contribute to the isotopologue ratio profile. In particular, in all models, there

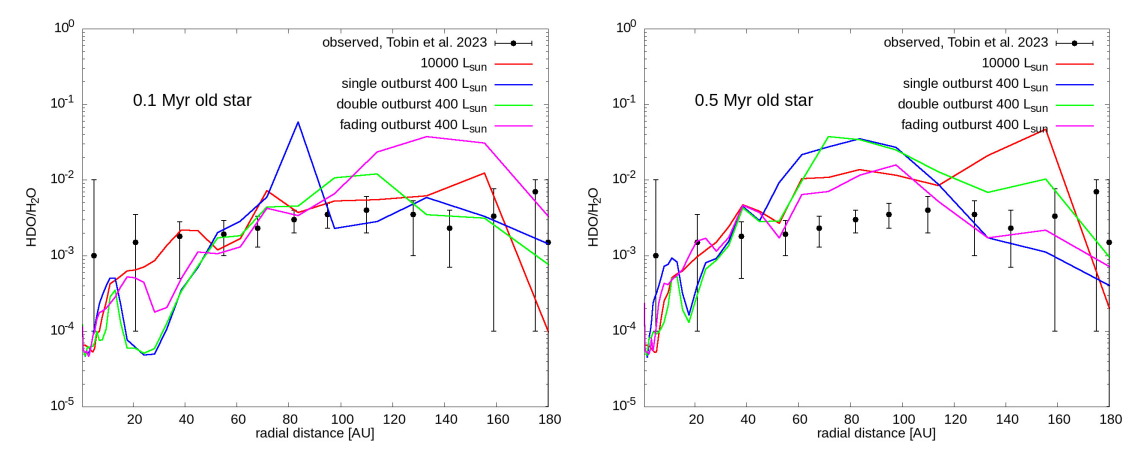


Figure 5. Comparison of model HDO/H₂O radial profiles for stellar ages of 0.1 and 0.5 M_{\odot} with observed data for V883 Ori (Tobin et al. 2023, black marks with error bars). The shown scenarios are: single 10,000 L_{\odot} outburst (blue line), single 400 L_{\odot} outburst (green line), the second outburst in the two 10,000 + 400 L_{\odot} outbursts scenario (red line), a fading 2000 L_{\odot} outburst at the moment when the luminosity is 400 L_{\odot} (purple line).

is a peak in the inner disk (at 10-40 au) that corresponds to the efficient formation of HDO in the molecular layer at $z/R \approx 0.2$ (reaction OH + HD \rightarrow HDO + H). This peak shifts with increasing accretion luminosity due to an increase in the OH abundance due to an increase in the temperature and radiation field.

For a 0.5 Myr old star, which has lower luminosity before the outburst, there is an additional increase in the HDO abundance in both the gas and ice phases at a distance of ${\sim}60$ -100 au (see Figure 3). This is reflected as an increase in the HDO/H₂O ratio in the profiles in Figure 4. In this region, the formation of water on dust grain surface is efficient, through the reaction GOH + GH \rightarrow GH_{2O} and its deuterated analogs. The efficiency of deuterated water formation on dust is sensitive to the temperature and density (Taquet et al. 2013), leading to differences in the HDO ice abundance in models with different stellar luminosity.

Thus, the pre-outburst luminosity also affects the HDO/H_2O ratio in the ice phase, which is reflected in the gas-phase HDO/H_2O during the outburst due to water ice evaporation. In this paper we consider two different values of stellar luminosity, but in reality an evolving protostar gradually changes luminosity, which should lead to a change in thermal structure even in the absence of luminosity outbursts.

For the least bright outburst ($400\,L_\odot$), the HDO/H₂O radial profile also shows a pronounced maximum at $\sim\!80$ au, similar to the one that in the pre-outburst phase is located at 50–60 au. At more powerful outbursts ($2000\,L_\odot$), the maximum is less pronounced and shifts to the outer regions of the protoplanetary disk (100-180 au), while at extreme luminosities ($10,000\,L_\odot$) the HDO/H₂O enhancement has a more homogeneous structure. The reaction of HDO formation in the gas phase in the protoplanetary disk plane is responsible for the HDO/H₂O enhancement in these regions, which has the most contribution for the $400\,L_\odot$ outburst of a $0.5\,\mathrm{Myr}$ old star.

HDO is formed from deuterated formaldehyde, HDCO, whose abundance is elevated relative to H_2CO . In turn, additional HDCO comes into the gas phase from the dust surface when the outburst vaporizes the icy HDCO present in these regions. This reaction has lower contribution in the models with brighter outbursts.

We show that high HDO/ $\rm H_2O$ values in FU Ori-type disks can persist even after multiple outbursts, which is consistent with the idea of transfer of inherited ice from the molecular cloud. This behavior may explain the observed elevated deuterium abundance in Hale–Bopp-type comets (3 \times 10⁻⁴ Meier et al. 1998), which confirms the connection between the early chemistry of protoplanetary disks and the composition of solar system bodies. We obtain similar to these cometary values in the inner disk, and the outer disks have even higher values.

3.3. Outburst Shape and the Effect of Past Changes in Luminosity

Although the current luminosity of V883 Ori is $\sim 400\,L_\odot$, the luminosity required to reproduce the observed HDO/H2O profiles on the order of $2000-10,000\,L_\odot$ may have been achieved in a previous more powerful outburst. In particular, a bright outburst may have occurred in the system in the past, leaving a trace in the form of snow line positions and a fraction of deuterated water that persists even at lower current luminosities. We consider a model in which two consecutive outbursts occur with amplitudes of 10,000 and $400\,L_\odot$ and compare HDO/H₂O during these different outbursts. We also consider a later time point at a fading stage of the outburst in the model with $L_{\rm acc} = 2000\,L_\odot$, when the accretion luminosity is also equal to $400\,L_\odot$. These scenarios represent possible options for the evolution of the luminosity. Since V883 Ori was not observed before the Connelley & Reipurth (2018)

outburst, the detailed history of the luminosity evolution is unknown, and the proposed scenarios could have occurred.

The results of the two-outburst model (Figure 5) demonstrate the complex dynamics of the HDO/H₂O ratio. The first powerful outburst (10,000 L_{\odot}) causes significant ice evaporation and changes in isotopic composition, while the subsequent outburst (400 L_{\odot}) further modifies the distribution. At the same time, the HDO/H₂O profile in this model is close to that of a single outburst at $10,\!000\,L_{\odot}$ and in agreement with the observational data. The main differences between these models lie in the region inside 50 au, where the observational data are less reliable. If we compare the two-outburst model with the single-outburst model of $400 L_{\odot}$ amplitude, we see the disappearance of the peak at 80 au, which deviates significantly from the observations. In the fading $2000 L_{\odot}$ outburst scenario, the HDO/H₂O at distances 80–140 au is much larger than observed. Similar behavior is observed in this model at the moment of the luminosity maximum (see Figure 4).

We can conclude that the model with two consecutive outbursts (Figure 5, red line) shows better agreement with the observed HDO/H₂O levels, particularly for the stellar luminosity corresponding to a 0.1 Myr old star. The effect of the past outburst persists in the outer parts of the protoplanetary disk over the considered time interval of $\sim 100 \ \rm yr$. The fraction of deuterated water is determined by the maximum luminosity in the recent past rather than by the current luminosity. In the absence of additional heating mechanisms and assuming an instantaneous change in the thermal structure of the disk, a bright ($\sim 10,000 \ L_{\odot}$) outburst in the past represents the most appropriate explanation for the observed radial HDO/H₂O distribution.

3.4. Alternative Temperature Profile

The key assumption of our modeling is the power-law dependence of the temperature on the radial distance and the luminosity of the central source. We assume the dependence where $T_{\rm mp} \propto L_{\rm acc}^{1/4} R^{-1/2}$, which is derived for fully optically thick protoplanetary disks (Dullemond et al. 2001). In our choice of the power law exponent q in the radial temperature profile $T_{\rm mp} \propto R^{-q}$ we rely on the observational data on protoplanetary disks that report $q \approx 0.5-0.6$ (e.g., Andrews et al. 2009). Similar temperature dependencies are used in many other astrochemical models of protoplanetary disks (e.g., Aikawa & Herbst 1999; Eistrup et al. 2016; Pacetti et al. 2025).

However, theoretical studies suggest that a more sophisticated calculation of the thermal structure can be crucial to determine the position of the snowline (Sasselov & Lecar 2000; Garaud & Lin 2007). In the models that account for disk flaring, viscous heating, the wavelength dependence of dust opacity, and radiative transfer in the vertical direction for not optically thick disks, the dust temperature in the midplane

often follows the relations $T_{\rm mp} \propto L_{\rm acc}^{2/7} R^{-3/7}$ (D'Alessio et al. 1998, 1999; Ida et al. 2016). The weak dependence on luminosity implies that a lower luminosity is sufficient to reach the same sublimation temperature at a given radius.

The use of an alternative temperature dependence could lead to the snowline position to be farther from the star at the $\approx 400\,L_{\odot}$ outburst. We test a model with the temperature defined by the empirical expression from Ida et al. (2016)

$$T_{\rm mp} = 150 \left(\frac{L_{\rm acc} + L_{\star}}{L_{\odot}}\right)^{2/7} \left(\frac{M_{\star}}{M_{\odot}}\right)^{-1/7} \times \left(\frac{R}{1 \text{ au}}\right)^{-3/7} \text{ K.}$$
(2)

The snowline position in this model is at $\approx 50\,\mathrm{au}$ for the $\approx 400\,L_\odot$ outburst, which is close to the observational limits of $40-100\,\mathrm{au}$. The HDO/H₂O ratio in this model is shown in Figure 6. It demonstrates a good agreement with the observations, and could be preferred over the results of the models with the classical temperature profile determined by Equation (1). Such temperature structure allows to simultaneously explain the observed snowline position and the profile of HDO/H₂O ratio with the current luminosity.

4. Discussion

The discrepancy between the observed luminosity of $400\,L_\odot$ and the position of the snow lines, as well as the best agreement of the observed HDO/H₂O profile with a $10,000\,L_\odot$ model, can be interpreted in different ways.

Modeling indicates that it is the evaporation of water ice as the temperature rises that determines the HDO/ $\rm H_2O$ ratio in the gas during the outburst in a large part of the disk, for which heating from an outburst of the observed amplitude of $400\,L_\odot$ is insufficient. This may be due to:

- 1. Insufficient consideration of additional heating sources (e.g., in the midplane of the disk) or simplified description of the temperature profile.
- 2. The influence of previous outbursts that changed the initial ice composition.
- 3. Nonlinear dynamics of chemical processes during outbursts.

In order to reproduce the observed high HDO/ $\rm H_2O$ ratio, it is necessary to transfer these molecules from the ice phase to the gas phase. However, the current accretion luminosity observed in V883 Ori is insufficient to vaporize the water ice in the distance range from 40 to 80 au. The additional temperature rise may arise from a brighter outburst (up to $10,000\,L_\odot$) that occurred in the recent past and has not been detected. The two-outburst model $(10,000+400\,L_\odot)$ most closely reproduces the observed HDO/ $\rm H_2O$ profiles in the V883 Ori disk, allowing us to explain the deuterated water fraction without the need for additional heating sources. The

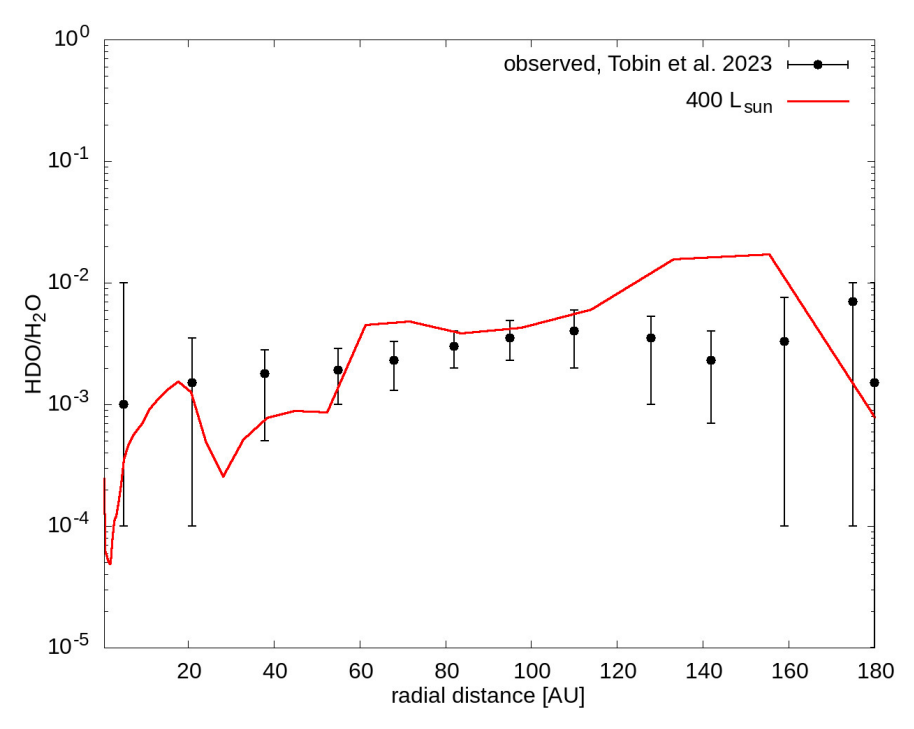


Figure 6. Radial profiles of the HDO/H₂O ratio in the gas for the model with temperature profile defined by Equation (2). Black marks with error bars show observational data for the V883 Ori protoplanetary disk from Tobin et al. (2023).

presence of a similar outburst in the past may also help explain the observed position of the water snow line, indirectly determined from the HCO⁺ emission (Leemker et al. 2021). Alternatively, a more sophisticated calculation of the temperature profile (e.g., Ida et al. 2016) allows to reproduce the observed snowline position and HDO/H₂O profile. Additional uncertainty is added by the time-dependent cooling of the protoplanetary disk after the end of the luminosity outburst: the characteristic heating and cooling times, especially in the dense regions of the disk, can exceed hundreds of years (Chiang & Goldreich 1997; Vorobyov et al. 2014).

Another restriction on the hypothesis of the bright past outburst is added by the required accretion rate. To reach the accretion luminosity of $10,000\,L_\odot$, the mass accretion rate to the star needs to be around $\frac{L_{\rm acc}R_*}{1.5GM_*}\approx 0.8\times 10^{-4}\,M_\odot\,{\rm yr}^{-1}$. During 100 yr of an outburst, around $0.01\,M_\odot$ will be accreted, which is around 20% of the adopted disk mass. A shorter duration of the burst could further ease this constraint. However, multiple such outbursts would sufficiently decrease the disk mass budget.

The hypothesis that radiative heating may not be the only source of heating in the protoplanetary disk cannot be discarded either. The inclusion of viscous heating may also help to push the water snow line further away from the star, as shown by Alarcón et al. (2024) modeling. At high accretion rates through the protoplanetary disk and in high-density disks, the zone of influence of accretion viscous heating can reach

distances of tens of astronomical units (Ueda et al. 2023). This mechanism may serve as an additional source of heating, providing an alternative to the bright outburst of luminosity in the past. The expected effect of such heating on the chemical composition is similar to the effect of enhanced radiative heating from an extremely bright luminosity outburst. To distinguish between these scenarios, constraints on the structure of the protoplanetary disk in the vertical direction are needed. Radiative heating primarily affects the upper layers of the disk, while accretion viscous heating is most effective in the disk midplane. Future ALMA observations targeting the highly excited HDO and H₂O lines, as well as planned mid-infrared ice band spectroscopy using JWST, will test these predictions by constraining the possible vertical distribution of water isotopologues in protoplanetary disks.

In addition to water, numerous deuterated isotopologues of various other molecules, including complex organic molecules, are also observed in the V883 Ori disk. These include deuterated formaldehyde (HDCO), methanol (CH₂DOH), acetaldehyde (CH₃CDO and CH₂DCHO), and methyl cyanide (CH₂DCN) (Lee et al. 2019, 2024). Upper limits on the D/H (Yamato et al. 2024) ratio were also obtained for some molecules. The diversity of observed complex organics, due to the outburst observed in the gas phase makes this FUor a unique object for studying chemistry in protoplanetary disks. Future more detailed numerical studies of the chemistry of deuterated species in disks around FUors are needed to

understand the observed diversity of molecules and the fractionation of deuterium between them.

5. Conclusions

In this work, we have numerically modeled the chemical composition of the protoplanetary disk around a young V883 Ori star experiencing a luminosity outburst. We modeled the radial distribution of the deuterated water fraction HDO/H2O and compared it with spatially resolved observational data (Tobin et al. 2023) for different luminosity change scenarios and for stellar luminosities corresponding to two ages (0.1 and $0.5 M_{\odot}$). We show that the closest agreement with observations is achieved in models where the maximum of the luminosity outburst is $\sim 10,000 L_{\odot}$ and $\sim 2000 L_{\odot}$. At the same time, models with lower luminosities corresponding to the current observed value (\sim 400 L_{\odot}) show HDO/H₂O above the observed value. An agreement of the observed luminosity \sim 400 L_{\odot} , approximate position of the snowline and the HDO/H₂O profile can be reached with the temperature dependence $T \propto R^{-3/7}$ (D'Alessio et al. 1998), which is not seen in the observed temperature profiles of protoplanetary disks (Andrews et al. 2009).

Our calculations show that the interpretation of the observed HDO/ $\rm H_2O$ distribution profiles is affected not only by the amplitude of the accretion luminosity outburst, but also by the age of the star and its corresponding luminosity. We considered two characteristic ages: 0.1 and 0.5 Myr, corresponding to different stages of protoplanetary disk evolution. The results (see for example, Figure 4) demonstrate that at higher stellar luminosities (corresponding to a younger age of 0.1 Myr) the profile becomes smoother, and the snow line position and water isotopologue abundances are more robust to changes in external conditions. More powerful outbursts such as 2000 and $10,000 \, L_{\odot}$, meanwhile, give better agreement with the observed data, especially at ages of 0.1 Myr, which may indicate the effect of previous outbursts or a change in the thermochemical structure of the protoplanetary disk with time.

Consideration of the two-outburst model shows that the effect of the brighter first outburst can persist for $\sim \! 100 \, \mathrm{yr}$, leading to an $\mathrm{HDO/H_2O}$ profile similar to the single-outburst case with $\sim \! 10,000 \, L_{\odot}$. This indicates that the system may have experienced a brighter luminosity outburst in the past, as previously proposed by Leemker et al. (2021). This hypothesis is also consistent with the positions of water snow lines determined from observations. However, we cannot exclude that such an effect could be caused by the presence of alternative heating sources instead of the brighter past outburst (Ueda et al. 2023; Alarcón et al. 2024).

These results emphasize the need to take into account the chemical heterogeneity of ice, the peculiarities of its radial and vertical distribution, and the residual effects of previous chemical evolution when interpreting the observed profiles of water isotopologues in FUor type objects.

Acknowledgments

The research was carried out under State Assignment FEUZ-2025-0003. Tamara Moryarova's work was supported by the Ministry of Science and Higher Education of the Russian Federation, State Assignment No. GZ0110/23-10-IF.

ORCID iDs

```
Anastasiia Topchieva https://orcid.org/0000-0003-0752-2082
Anton Vasyunin https://orcid.org/0000-0003-1684-3355
```

References

```
Aikawa, Y., & Herbst, E. 1999, A&A, 351, 233
Akimkin, V., Zhukovska, S., Wiebe, D., et al. 2013, ApJ, 766, 8
Alarcón, F., Casassus, S., Lyra, W., Pérez, S., & Cieza, L. 2024, MNRAS,
   527, 9655
Albertsson, T., Semenov, D. A., Vasyunin, A. I., Henning, T., & Herbst, E.
  2013, ApJS, 207, 27
Andreu, A., Coutens, A., Cruz-Sáenz de Miera, F., et al. 2023, A&A, 677, L17
Andrews, S. M., Wilner, D. J., Hughes, A. M., Qi, C., & Dullemond, C. P.
  2009, ApJ, 700, 1502
Bergin, E. A., Aikawa, Y., Blake, G. A., & van Dishoeck, E. F. 2007, in
  Protostars and Planets V, ed. B. Reipurth, D. Jewitt, & K. Keil (Tucson:
  Univ. of Arizona Press), 751
Carvalho, A. S., Hillenbrand, L. A., & Kóspál, Á. 2025, ApJ, 993, 38
Chiang, E. I., & Goldreich, P. 1997, ApJ, 490, 368
Cieza, L. A., Casassus, S., Tobin, J., et al. 2016, Natur, 535, 258
Cieza, L. A., Ruíz-Rodríguez, D., Perez, S., et al. 2018, MNRAS, 474, 4347
Cleeves, L. I., Bergin, E. A., Alexander, C. M. O. D., et al. 2014, Sci,
  345, 1590
Connelley, M. S., & Reipurth, B. 2018, ApJ, 861, 145
D'Alessio, P., Calvet, N., Hartmann, L., Lizano, S., & Cantó, J. 1999, ApJ,
D'Alessio, P., Cantö, J., Calvet, N., & Lizano, S. 1998, ApJ, 500, 411
Drążkowska, J., & Alibert, Y. 2017, A&A, 608, A92
Dullemond, C. P., Dominik, C., & Natta, A. 2001, ApJ, 560, 957
Eistrup, C., Walsh, C., & van Dishoeck, E. F. 2016, A&A, 595, A83
Evans, N. J., II, Dunham, M. M., Jørgensen, J. K., et al. 2009, ApJS, 181, 321
Furlan, E., Fischer, W. J., Ali, B., et al. 2016, ApJS, 224, 5
Furuya, K., Aikawa, Y., Nomura, H., Hersant, F., & Wakelam, V. 2013, ApJ,
Furuya, K., van Dishoeck, E. F., & Aikawa, Y. 2016, A&A, 586, A127
Garaud, P., & Lin, D. N. C. 2007, ApJ, 654, 606
Houge, A., & Krijt, S. 2023, MNRAS, 521, 5826
Houge, A., Macías, E., & Krijt, S. 2023, MNRAS, 527, 9668
Harsono, D., Bruderer, S., & van Dishoeck, E. F. 2015, A&A, 582, A41
Ida, S., Guillot, T., & Morbidelli, A. 2016, A&A, 591, A72
Isella, A., Guidi, G., Testi, L., et al. 2016, PhRvL, 117, 251101
Jacquet, E., & Robert, F. 2013, Icar, 223, 722
Kamp, I., & Dullemond, C. P. 2004, ApJ, 615, 991
Kirsanova, M. S., Baklanov, P. V., Vasiliev, E. O., et al. 2025, PhyU, 68, 278
Kóspál, Á., Cruz-Sáenz de Miera, F., White, J. A., et al. 2021, ApJS, 256, 30
Laor, A., & Draine, B. T. 1993, ApJ, 402, 441
Lee, J.-E., Kim, C.-H., Lee, S., et al. 2024, ApJ, 966, 119
Lee, J.-E., Lee, S., Baek, G., et al. 2019, NatAs, 3, 314
Leemker, M., van't Hoff, M. L. R., Trapman, L., et al. 2021, A&A, 646, A3
Meier, R., Owen, T. C., Matthews, H. E., et al. 1998, Sci, 279, 842
Molyarova, T., Akimkin, V., Semenov, D., et al. 2017, ApJ, 849, 130
Molyarova, T., Akimkin, V., Semenov, D., et al. 2018, ApJ, 866, 46
Molyarova, T. S., & Elbakyan, V. G. 2019, INASR, 4, 45
```

```
Müller, J., Savvidou, S., & Bitsch, B. 2021, A&A, 650, A185
Öberg, K. I., Boogert, A. C. A., Pontoppidan, K. M., et al. 2011, ApJ, 740, 109
Owen, J. E., & Jacquet, E. 2015, MNRAS, 446, 3285
Pacetti, E., Schisano, E., Turrini, D., et al. 2025, A&A, 701, A194
Pickering, E. C. 1890, AnHar, 18, 1
Sandell, G., & Weintraub, D. A. 2001, ApJS, 134, 115
Sasselov, D. D., & Lecar, M. 2000, ApJ, 528, 995
Schoonenberg, D., Okuzumi, S., & Ormel, C. W. 2017, A&A, 605, L2
Semenov, D., & Wiebe, D. 2011, ApJS, 196, 25
Strom, K. M., & Strom, S. E. 1993, ApJL, 412, L63
Taquet, V., Peters, P. S., Kahane, C., et al. 2013, A&A, 550, A127
Tobin, J. J., van't Hoff, M. L. R., Leemker, M., et al. 2023, Natur, 615, 227
Ueda, T., Okuzumi, S., Kataoka, A., & Flock, M. 2023, A&A, 675, A176
```

```
Vorobyov, E. I., Pavlyuchenkov, Y. N., & Trinkl, P. 2014, ARep, 58, 522
Whitney, B. A., Wood, K., Bjorkman, J. E., & Wolff, M. J. 2003, ApJ, 591, 1049
Wiebe, D. S., Molyarova, T. S., Akimkin, V. V., Vorobyov, E. I., & Semenov, D. A. 2019, MNRAS, 485, 1843
Williams, J. P., & Best, W. M. J. 2014, ApJ, 788, 59
Wilson, T. L., & Rood, R. 1994, ARA&A, 32, 191
Woitke, P., Kamp, I., & Thi, W. F. 2009, A&A, 501, 383
Yamato, Y., Notsu, S., Aikawa, Y., et al. 2024, AJ, 167, 66
Yorke, H. W., & Bodenheimer, P. 2008, in ASP Conf. Ser. 387, Massive Star
```

Formation: Observations Confront Theory, ed. H. Beuther, H. Linz, &